Aerospace Science and Technology 25 (2013) 177–189

Contents lists available at SciVerse ScienceDirect

Aerospace Science and Technology

www.elsevier.com/locate/aescte

Improving variable-fidelity surrogate modeling via gradient-enhanced kriging and a generalized hybrid bridge function

Zhong-Hua Han [a,*,1], Stefan Görtz [b,2], Ralf Zimmermann [b,2]

[a] National Key Laboratory of Science and Technology on Aerodynamic Design and Research, Department of Fluid Mechanics, School of Aeronautics, Northwestern Polytechnical University, 710072 Xi'an, PR China
[b] German Aerospace Center (DLR), D-38108 Braunschweig, Germany

ARTICLE INFO

Article history:
Received 12 February 2011
Received in revised form 4 January 2012
Accepted 5 January 2012
Available online 21 January 2012

Keywords:
Surrogate model
Variable-fidelity model
Kriging model
Computational fluid dynamics

ABSTRACT

Variable-fidelity surrogate modeling offers an efficient way to generate aerodynamic data for aero-loads prediction based on a set of CFD methods with varying degree of fidelity and computational expense. In this paper, direct Gradient-Enhanced Kriging (GEK) and a newly developed Generalized Hybrid Bridge Function (GHBF) have been combined in order to improve the efficiency and accuracy of the existing Variable-Fidelity Modeling (VFM) approach. The new algorithms and features are demonstrated and evaluated for analytical functions and are subsequently used to construct a global surrogate model for the aerodynamic coefficients and drag polar of an RAE 2822 airfoil. It is shown that the gradient-enhanced GHBF proposed in this paper is very promising and can be used to significantly improve the efficiency, accuracy and robustness of VFM in the context of aero-loads prediction.

1. Introduction

From an aerodynamic point of view, an aircraft is defined by comprehensive datasets regarding performance, loads and handling characteristics. This data, which needs to be determined at a given timescale and cost for every possible flight condition and aircraft configuration, is used to design the structure of the aircraft and the flight control system. Currently, this data is obtained mainly from costly wind tunnel tests or by using hand-book methods. The use of higher-fidelity and thus more accurate but also more time consuming CFD methods has been, up to now, impossible due to the large number of load cases that need to be evaluated to achieve aircraft certification. Only a subset of the required data can be computed with high-fidelity CFD at present. The "brute-force" approach of computing all relevant data with high-fidelity CFD is currently not feasible and methods for reducing the computational costs are sought after.

The long-term goal of the work described herein is the development of a process chain for the efficient numerical prediction of all certification-relevant aerodynamic data for the elastic aircraft over the full flight envelope, based on a hierarchy of CFD methods from low to high fidelity. The idea is to use Variable-Fidelity Modeling (VFM) to produce this data in a reduced time-frame with guaranteed accuracy and minimum computational effort.

The VFM method [1,2] for aero-loads prediction uses a set of CFD methods with varying degrees of fidelity and computational expense (potential theory, Euler equations, and RANS equations) or a single physical model evaluated on meshes of varying refinement to approximate the unknown aerodynamic data as a function of input parameters such as Mach number, angle of attack, etc., while reducing the number of expensive high-fidelity computations. VFM as discussed in this paper has the same meaning as "multi-fidelity modeling", "variable-complexity modeling", "data fusion" or "data merging".

The most popular method currently used for VFM is a correction-based method. The correction is called "bridge function", "scaling function" or "calibration". The correction can be multiplicative, additive or hybrid multiplicative/additive. Multiplicative bridge function was used for variable-fidelity optimization [3] since 1993. It is used to "locally" scale the low-fidelity function to approximate the high-fidelity function. When it is combined with the trust region method [4–6], the optimization cost can be greatly reduced. Additive bridge function was then developed as an "global" correction and has become the most popular method for variable-fidelity optimization [7–9] or for data fusion [10]. It was proven to be more accurate and robust than a multiplicative bridge function. To represent more complicated correlation between low- and high-fidelity functions, a hybrid multiplicative/additive bridge function method was proposed in [11–13] for variable-fidelity optimization. A VFM framework for aero-loads prediction was developed by the authors as described in Refs. [1,2]. It was verified

* Corresponding author.
E-mail addresses: hanzh@nwpu.edu.cn (Z.-H. Han), Stefan.Goertz@dlr.de (S. Görtz), Ralf.Zimmermann@dlr.de (R. Zimmermann).

[1] Research Scientist, former affiliation: German Aerospace Center (DLR), Institute of Aerodynamics and Flow Technology, $C^2A^2S^2E$.

[2] Research Scientist, Institute of Aerodynamics and Flow Technology, $C^2A^2S^2E$.

1270-9638/$ – see front matter
doi:10.1016/j.ast.2012.01.006

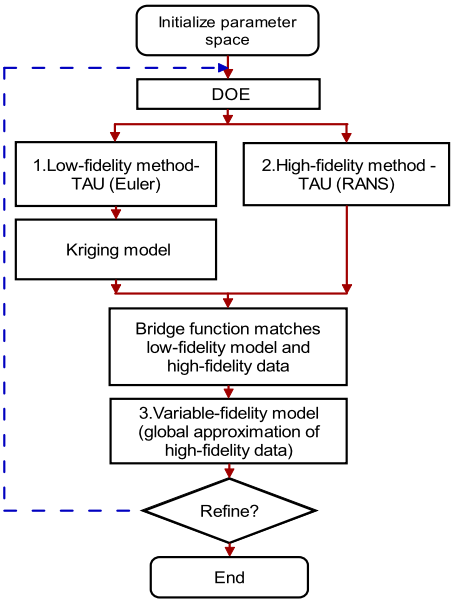

Fig. 1. VFM framework for aero-loads prediction.

for analytic problems and preliminarily demonstrated and evaluated for the construction of global approximation models of the aerodynamic coefficients and drag polar of a 2D airfoil. It was demonstrated that the approximation method, the bridge function and the refinement strategy are the key elements for constructing a VFM model. Although the VFM method has been shown to be promising, more research has to be carried out to develop new methods and technologies that will further improve its efficiency, accuracy and robustness.

Aware of the importance of improving the available VFM algorithm in the context of aero-loads prediction, this paper focuses on Gradient-Enhanced Kriging (GEK) in combination with a new Generalized Hybrid Bridge Function (GHBF) methodology. The new methods and technologies are verified for analytic problems and demonstrated by constructing a global approximation model for the aerodynamic coefficients and the drag polar of an RAE 2822 airfoil.

The paper is organized as follows: Section 2 gives a brief overview of the framework of the VFM method we are concerned with. Section 3 deals with the details of the GEK method, including the GEK predictor and its Mean Squared Error (MSE), the choice of the correlation models, model fitting and remarks on the difference between GEK and cokriging. Section 4 is about the development of the GHBF for VFM. Finally, Section 5 shows some numerical examples.

2. Variable-fidelity modeling framework

This article focuses on the development of a VFM method that is especially well suited for predicting and modeling the aerodynamic data of aircraft throughout their full flight envelope. VFM is essentially a model management methodology. It uses a set of CFD methods with varying degrees of fidelity and computational expense or a single physical model evaluated on meshes of varying resolutions. A low-fidelity CFD method is used to automatically compute hundreds or thousands of solutions at points in the parameter space selected with a Design of Experiments (DoE) tool. The remainder of the parameter space is "filled in" using interpolation procedures. A few points in the parameter space are computed using a high-fidelity CFD method. These points are also selected using a DoE tool. Then, data fusion is used to combine the data stemming from the different methods, with low-fidelity data indicating trends and a small number of high-fidelity data correcting the absolute values. This is done by using so-called bridge functions. The model is adaptively refined by inserting additional samples based on various refinement criteria. The VFM framework was designed for constructing a model that can approximate the high-fidelity data throughout the parameter space. A flow chart is depicted in Fig. 1. The basic steps of this framework are as follows:

- *Step 1 – Initialization*: Define the unknown aerodynamic function (integrated or distributed) to be modeled; specify the parameter space by defining the independent variables and their range.
- *Step 2 – Sampling*: Two sets of sample points (called samples in the following) are generated based on Design-of-Experiment (DoE) theory; one set with a large number of samples to be evaluated with the low-fidelity method and one significantly smaller set for evaluation with the high-fidelity method.
- *Step 3 – Sample point evaluation*: The aerodynamic data at the samples are calculated with the low- and high-fidelity CFD methods, respectively.
- *Step 4 – Low-fidelity surrogate model and bridge function*: Based on the sampled low-fidelity data, a kriging model is constructed as a surrogate model to the low-fidelity CFD method (called low-fidelity kriging model). Based on the difference between the low-fidelity surrogate model and the high-fidelity data at the locations of the high-fidelity samples, a kriging-based bridge function is constructed to match the low- and high-fidelity CFD methods.
- *Step 5 – Initial VFM construction*: The low-fidelity surrogate model is corrected with the bridge function and an initial VFM is constructed.
- *Step 6 – Refinement*: iterative refinement is performed by adding additional samples until a criterion for termination is fulfilled.
- *Step 7 – Final VFM for aero-loads prediction*: Based on the final VFM, the parameter space can be probed in "real-time" for aerodynamic data at any point in the parameter space within the limits prescribed in Step 1 or a database of aerodynamic data can be efficiently generated by filling in the remainder of the parameter space using the VFM.

3. Gradient-enhanced kriging

Kriging is a statistical interpolation method suggested by Krige [14] in 1951 and mathematically formulated by Matheron [15] in 1963. Kriging estimation depends on the spatial correlations between given sample points to be interpolated. Gradient-Enhanced Kriging (GEK) denotes the extension of kriging to models where the gradient information is incorporated into the construction of the kriging model to improve the accuracy of the prediction for a given number of samples. In turn, the efficiency of constructing an approximation model for an unknown aerodynamic function can be improved as fewer samples are needed for a given level of accuracy. There are two ways to incorporate the gradient information at samples, which lead to two different methods: direct GEK and indirect GEK (see Refs. [16,17]).

In the case of direct GEK [20–22], the gradient information is directly included in the kriging equation system by adding the weighted sum of the gradients to the weighted sum of the data. The additional weights are calculated by changing the kriging equation system to include the correlation between the data and the gradients. These correlations are modeled by differentiating the correlation function. A formal mathematical derivation of the kriging equation system and construction of the correlation function as well as correlation vector are necessary. In contrast to indirect GEK, where a finite difference step size has to be determined for

exploiting derivative information [18,19], no additional parameters are involved in the direct GEK formulation. In addition, direct GEK is more accurate in theory as no numerical error is introduced due to the step size. Note that direct GEK is not a completely new method.

Since few publications on direct GEK can be found in the literature (see Refs. [16–22]), we present an independently derived, self-contained formulation of the direct GEK method as well as some implementation issues in the following.

Recall that for the derivation of a kriging model [23], it is assumed that the sampled dataset $(\mathbf{S}, \mathbf{y}_S)$ for an m-dimensional problem with n samples is of the form

$$\mathbf{S} = \begin{bmatrix} \mathbf{x}^{(1)} \\ \mathbf{x}^{(2)} \\ \vdots \\ \mathbf{x}^{(n)} \end{bmatrix} = \begin{bmatrix} x_1^{(1)} & x_2^{(1)} & \cdots & x_m^{(1)} \\ x_1^{(2)} & x_2^{(2)} & \cdots & x_m^{(2)} \\ \vdots & \vdots & \ddots & \vdots \\ x_1^{(n)} & x_2^{(n)} & \cdots & x_m^{(n)} \end{bmatrix} \in \mathbb{R}^{n\times m},$$

$$\mathbf{y}_S = \begin{bmatrix} y^{(1)} \\ y^{(2)} \\ \vdots \\ y^{(n)} \end{bmatrix} \in \mathbb{R}^n, \tag{1}$$

where $\mathbf{S}$ is a matrix with each row vector representing a sample location, and $\mathbf{y}_S$ is the column vector that contains the function value at each sample. Note that the goal of constructing an approximation model is to get the response of y at any untried $\mathbf{x}$ based on the sampled dataset $(\mathbf{S}, \mathbf{y}_S)$.

For the derivation of GEK, the column vector of observed data is extended to include the gradient information at the sample sites in the form of partial derivatives. Then the definition of $\mathbf{S}$ and $\mathbf{y}_S$ changes to

$$\begin{aligned} \mathbf{S} &= \left[\mathbf{x}^{(1)}, \ldots, \mathbf{x}^{(n)}, \mathbf{x}_g^{(1)}, \ldots, \mathbf{x}_g^{(n')}\right]^{\mathrm{T}} \in \mathbb{R}^{(n+n')\times m}, \\ \mathbf{y}_S &= \left[y^{(1)}, \ldots, y^{(n)}, \partial y^{(1)}, \ldots, \partial y^{(n')}\right]^{\mathrm{T}} \in \mathbb{R}^{n+n'}, \end{aligned} \tag{2}$$

where $\mathbf{x}_g^{(j)}$, $j \in \{1, \ldots, n'\}$ represents the location at which the jth partial derivative is enforced, and the entry $\partial y^{(j)} = (\frac{\partial y}{\partial x_k})^{(j)}$ in the vector $\mathbf{y}_S$ is the corresponding jth partial derivative (w.r.t. the kth independent variable, $k \in \{1, \ldots, m\}$). Note that in the present derivation, we do not assume that the gradient information is available at every sample site or in every parameter direction. In other words, the number of total partial derivatives n' can be less than $n \cdot m$. This assumption is reasonable as probably the gradient information is not available for some sample locations. For convenience, we drop the subscript "g" in $\mathbf{x}_g^{(j)}$ in the text below.

3.1. GEK predictor and MSE

Note that here the derivation of GEK is based on "ordinary" kriging. The extension to "universal" kriging is straightforward and will not be discussed here.

For a stationary random process, the statistical prediction of the unknown function y (e.g. the output of a computer code) at an untried $\mathbf{x}$ is given by a linear combination of the function values at the original samples and their gradients at observed points as follows

$$\hat{y}(\mathbf{x}) = \sum_{i=1}^{n} w^{(i)} y^{(i)} + \sum_{j=1}^{n'} \lambda^{(j)} \partial y^{(j)}, \quad \mathbf{x} \in \mathbb{R}^m, \tag{3}$$

where $\hat{y}(\mathbf{x})$ is the predicted value at an untried site $\mathbf{x}$, $w^{(i)}$ are the weight coefficients for function values $y^{(i)}$, and $\lambda^{(j)}$ are the weight coefficients for the partial derivatives, which have the same physical dimension as $(w\Delta x_k)$. Note that in our derivation the number of function values and the number of derivatives can be arbitrary, and the location where derivatives are enforced is also arbitrary. As with the kriging predictor in [23], the output of a deterministic computer experiment is treated as a realization of a random function (or stochastic process). Hence, we replace $\mathbf{y}_S = [y^{(1)}, \ldots, y^{(n)}, \partial y^{(1)}, \ldots, \partial y^{(n')}]^{\mathrm{T}}$ with the corresponding random quantities and assume

$$Y(\mathbf{x}) = \beta_0 + Z(\mathbf{x}) \tag{4}$$

with $\beta_0 \in \mathbb{R}^1$ being its unknown constant mean value and the stationary random processes $Z(\cdot)$ having zero mean and a covariance of

$$\begin{aligned} &Cov\left[Z\left(\mathbf{x}^{(i)}\right), Z\left(\mathbf{x}^{(j)}\right)\right] = \sigma^2 R\left(\mathbf{x}^{(i)}, \mathbf{x}^{(j)}\right), \\ &Cov\left[Z\left(\mathbf{x}^{(i)}\right), \frac{\partial Z(\mathbf{x}^{(j)})}{\partial x_k}\right] = \sigma^2 \frac{\partial R(\mathbf{x}^{(i)}, \mathbf{x}^{(j)})}{\partial x_k^{(j)}}, \\ &Cov\left[\frac{\partial Z(\mathbf{x}^{(i)})}{\partial x_k}, Z\left(\mathbf{x}^{(j)}\right)\right] = \sigma^2 \frac{\partial R(\mathbf{x}^{(i)}, \mathbf{x}^{(j)})}{\partial x_k^{(i)}}, \\ &Cov\left[\frac{\partial Z(\mathbf{x}^{(i)})}{\partial x_l}, \frac{\partial Z(\mathbf{x}^{(j)})}{\partial x_k}\right] = \sigma^2 \frac{\partial^2 R(\mathbf{x}^{(i)}, \mathbf{x}^{(j)})}{\partial x_l^{(i)} \partial x_k^{(j)}}. \end{aligned} \tag{5}$$

Here, σ^2 is the process variance of $Z(\cdot)$, R is the spatial correlation function, which is only dependent on the spatial distance between two sites. Note that $\frac{\partial R(\mathbf{x}^{(i)}, \mathbf{x}^{(j)})}{\partial x_k^{(i)}}$ and $\frac{\partial R(\mathbf{x}^{(i)}, \mathbf{x}^{(j)})}{\partial x_k^{(j)}}$ are the partial derivatives w.r.t. the kth component of $\mathbf{x}^{(i)}$ and $\mathbf{x}^{(j)}$, respectively. We also treat $\hat{y}(\mathbf{x})$ as random, and try to minimize its Mean Squared Error (MSE)

$$\mathrm{MSE}\left[\hat{y}(\mathbf{x})\right] = E\left[\left(\sum_{i=1}^{n} w^{(i)} Y^{(i)} + \sum_{j=1}^{n'} \lambda^{(j)} \partial Y^{(j)} - Y(\mathbf{x})\right)^2\right], \tag{6}$$

subject to the unbiasedness constraint

$$E\left[\sum_{i=1}^{n} w^{(i)} Y^{(i)} + \sum_{j=1}^{n'} \lambda^{(j)} \partial Y^{(j)}\right] = E\left[Y(\mathbf{x})\right]. \tag{7}$$

Solving this constrained minimization problem, $w^{(i)}$ and $\lambda^{(j)}$ in Eq. (3) can be found by solving the following linear equations

$$\begin{cases} \displaystyle\sum_{j=1}^{n} w^{(j)} Cov\left[Z\left(\mathbf{x}^{(i)}\right), Z\left(\mathbf{x}^{(j)}\right)\right] \\ \qquad \displaystyle + \sum_{j=1}^{n'} \lambda^{(j)} Cov\left[Z\left(\mathbf{x}^{(i)}\right), \frac{\partial Z(\mathbf{x}^{(j)})}{\partial x_k}\right] + \frac{\mu}{2} \\ \quad = Cov\left[Z\left(\mathbf{x}^{(i)}\right), Z(\mathbf{x})\right], \quad i = 1, \ldots, n, \\ \displaystyle\sum_{i=1}^{n} w^{(i)} Cov\left[\frac{\partial Z(\mathbf{x}^{(j)})}{\partial x_k}, Z\left(\mathbf{x}^{(i)}\right)\right] \\ \qquad \displaystyle + \sum_{i=1}^{n'} \lambda^{(i)} Cov\left[\frac{\partial Z(\mathbf{x}^{(j)})}{\partial x_k}, \frac{\partial Z(\mathbf{x}^{(i)})}{\partial x_l}\right] \\ \quad = Cov\left[\frac{\partial Z(\mathbf{x}^{(j)})}{\partial x_k}, Z(\mathbf{x})\right], \quad j = 1, \ldots, n', \\ \displaystyle\sum_{i=1}^{n} w^{(i)} = 1, \end{cases} \tag{8}$$

where μ is the Lagrange multiplier used to change the constrained minimization of the mean squared error into an unconstrained one, which in turn is necessary to fulfill the unbiasedness condition. Substituting Eq. (5) in Eq. (8) leads to the following linear equations

$$\begin{cases} \sum_{j=1}^{n} w^{(j)} R\big(\mathbf{x}^{(i)}, \mathbf{x}^{(j)}\big) + \sum_{j=1}^{n'} \lambda^{(j)} \frac{\partial R(\mathbf{x}^{(i)}, \mathbf{x}^{(j)})}{\partial x_k^{(j)}} + \frac{\mu}{2\sigma^2} \\ \quad = R\big(\mathbf{x}^{(i)}, \mathbf{x}\big), \quad i = 1, \ldots, n, \\ \sum_{i=1}^{n} w^{(i)} \frac{\partial R(\mathbf{x}^{(j)}, \mathbf{x}^{(i)})}{\partial x_k^{(j)}} + \sum_{i=1}^{n'} \lambda^{(i)} \frac{\partial^2 R(\mathbf{x}^{(j)}, \mathbf{x}^{(i)})}{\partial x_k^{(j)} \partial x_l^{(i)}} \\ \quad = \frac{\partial R(\mathbf{x}^{(j)}, \mathbf{x})}{\partial x_k^{(j)}}, \quad j = 1, \ldots, n', \\ \sum_{i=1}^{n} w^{(i)} = 1, \end{cases} \tag{9}$$

or in matrix form

$$\begin{bmatrix} \mathbf{R} & \mathbf{F} \\ \mathbf{F}^{\mathrm{T}} & 0 \end{bmatrix} \begin{bmatrix} \mathbf{w} \\ \tilde{\mu} \end{bmatrix} = \begin{bmatrix} \mathbf{r} \\ 1 \end{bmatrix}, \tag{10}$$

where

$$\mathbf{F} = (\underbrace{1, \ldots, 1}_{n}, \underbrace{0, \ldots, 0}_{n'})^{\mathrm{T}},$$

$$\mathbf{w} = \big(w^{(1)}, \ldots, w^{(n)}, \lambda^{(1)}, \ldots, \lambda^{(n')}\big)^{\mathrm{T}}, \qquad \tilde{\mu} = \mu / \big(2\sigma^2\big). \tag{11}$$

$\mathbf{R}$ is the correlation matrix representing the correlation between the observed points, and $\mathbf{r}$ is the correlation vector representing the correlation between the untried point and the observed points. If the number of derivatives and the number of the locations at which the gradient information is enforced are both arbitrary for a high-dimensional problem, the expressions for $\mathbf{R}$ and $\mathbf{r}$ are difficult to write down. Here, for convenience, the correlation matrix and correlation vector are written down for a one-dimensional problem with n function values and the corresponding n partial derivatives:

$$\mathbf{R} = \begin{bmatrix} R(x^{(1)}, x^{(1)}) & \cdots & R(x^{(1)}, x^{(n)}) & \frac{\partial R(x^{(1)}, x^{(1)})}{\partial x^{(1)}} & \cdots & \frac{\partial R(x^{(1)}, x^{(n)})}{\partial x^{(n)}} \\ \vdots & \ddots & \vdots & \vdots & \ddots & \vdots \\ R(x^{(n)}, x^{(1)}) & \cdots & R(x^{(n)}, x^{(n)}) & \frac{\partial R(x^{(n)}, x^{(1)})}{\partial x^{(1)}} & \cdots & \frac{\partial R(x^{(n)}, x^{(n)})}{\partial x^{(n)}} \\ \frac{\partial R(x^{(1)}, x^{(1)})}{\partial x^{(1)}} & \cdots & \frac{\partial R(x^{(1)}, x^{(n)})}{\partial x^{(1)}} & \frac{\partial^2 R(x^{(1)}, x^{(1)})}{\partial^2 x^{(1)}} & \cdots & \frac{\partial^2 R(x^{(1)}, x^{(n)})}{\partial x^{(1)} \partial x^{(n)}} \\ \vdots & \ddots & \vdots & \vdots & \ddots & \vdots \\ \frac{\partial R(x^{(n)}, x^{(1)})}{\partial x^{(n)}} & \cdots & \frac{\partial R(x^{(n)}, x^{(n)})}{\partial x^{(n)}} & \frac{\partial^2 R(x^{(n)}, x^{(1)})}{\partial x^{(n)} \partial x^{(1)}} & \cdots & \frac{\partial^2 R(x^{(n)}, x^{(n)})}{\partial^2 x^{(n)}} \end{bmatrix},$$

$$\mathbf{r} = \begin{bmatrix} R(x^{(1)}, x) \\ \vdots \\ R(x^{(n)}, x) \\ \frac{\partial R(x^{(1)}, x)}{\partial x^{(1)}} \\ \vdots \\ \frac{\partial R(x^{(n)}, x)}{\partial x^{(n)}} \end{bmatrix}. \tag{12}$$

Computing the optimal weight coefficients $w^{(i)}$ and $\lambda^{(j)}$ leads to the GEK predictor for any untried $\mathbf{x}$:

$$\hat{y}(\mathbf{x}) = \begin{bmatrix} \mathbf{r}(\mathbf{x}) \\ 1 \end{bmatrix}^{\mathrm{T}} \begin{bmatrix} \mathbf{R} & \mathbf{F} \\ \mathbf{F}^{\mathrm{T}} & 0 \end{bmatrix}^{-1} \begin{bmatrix} \mathbf{y}_{\mathrm{S}} \\ 0 \end{bmatrix}. \tag{13}$$

By inverting the partitioned matrix, the GEK predictor can be written in a form with which the reader may be more familiar

$$\hat{y}(\mathbf{x}) = \beta_0 + \mathbf{r}^{\mathrm{T}}(\mathbf{x}) \underbrace{\mathbf{R}^{-1}(\mathbf{y}_{\mathrm{S}} - \beta_0 \mathbf{F})}_{=:\mathbf{v}_{\mathrm{GEK}}}, \tag{14}$$

where $\beta_0 = (\mathbf{F}^{\mathrm{T}}\mathbf{R}^{-1}\mathbf{F})^{-1}\mathbf{F}^{\mathrm{T}}\mathbf{R}^{-1}\mathbf{y}_{\mathrm{S}}$. Note that the vector $\mathbf{V}_{\mathrm{GEK}} \in \mathbb{R}^{n+n'}$ only depends on the observed values (both function values and gradients), and it can be calculated at the model fitting stage of a GEK model. Once $\mathbf{V}_{\mathrm{GEK}}$ is obtained, the prediction of the unknown function value y at any untried $\mathbf{x}$ only requires re-calculating $\mathbf{r}^{\mathrm{T}}(\mathbf{x})$. Based on the GEK predictor, the unknown gradient $\partial y / \partial x_k$ at an untried $\mathbf{x}$ can be estimated with the following "gradient predictor"

$$\frac{\partial \hat{y}(\mathbf{x})}{\partial x_k} = \frac{\partial}{\partial x_k}\big[\mathbf{r}^{\mathrm{T}}(\mathbf{x})\big] \underbrace{\mathbf{R}^{-1}(\mathbf{y}_{\mathrm{S}} - \beta_0 \mathbf{F})}_{=:\mathbf{v}_{\mathrm{GEK}}}, \tag{15}$$

where $\frac{\partial}{\partial x_k}[\mathbf{r}^{\mathrm{T}}(\mathbf{x})]$ can be obtained by differentiating the correlation function in the same way as in Eq. (5). With the above formula, it can be verified if the GEK predictor exactly reproduces the partial derivatives prescribed by the sample data. There are a couple of applications for the gradient predictor in Eq. (15). It can, for example, be used to estimate the derivatives related to the stability and control of an aircraft or implement sensitive analysis for a design problem.

The MSE of the GEK prediction is proven to be

$$\begin{aligned} &\mathrm{MSE}\big\{\hat{y}(\mathbf{x})\big\} \\ &\quad = \sigma^2 \left\{ 1.0 - \begin{bmatrix} \mathbf{r} \\ 1 \end{bmatrix}^{\mathrm{T}} \begin{bmatrix} \mathbf{R} & \mathbf{F} \\ \mathbf{F}^{\mathrm{T}} & 0 \end{bmatrix}^{-1} \begin{bmatrix} \mathbf{r} \\ 1 \end{bmatrix} \right\} \\ &\quad = \sigma^2 \big\{ 1.0 - \mathbf{r}^{\mathrm{T}}\mathbf{R}^{-1}\mathbf{r} + \big(\mathbf{r}^{\mathrm{T}}\mathbf{R}^{-1}\mathbf{F} - 1\big)^2 / \big(\mathbf{F}^{\mathrm{T}}\mathbf{R}^{-1}\mathbf{F}\big) \big\}. \end{aligned} \tag{16}$$

3.2. Correlation models

The construction of the correlation matrix $\mathbf{R}$ and the correlation vector $\mathbf{r}$ requires the calculation of the correlation function as well as its first and second derivatives. The correlation function for random variables at two sites $\mathbf{x}^{(i)}, \mathbf{x}^{(j)}$, is assumed to only depend on the spatial distance (namely $R(\mathbf{x}^{(i)}, \mathbf{x}^{(j)}) = R(\mathbf{x}^{(i)} - \mathbf{x}^{(j)})$). Here we focus on a family of correlation models that are of the form

$$R\big(\mathbf{x}^{(i)}, \mathbf{x}^{(j)}\big) = \prod_{k=1}^{m} R_k\big(\theta_k, \mathbf{x}^{(i)} - \mathbf{x}^{(j)}\big). \tag{17}$$

The correlation functions used in this article are defined as follows:

- "GAUSS" correlation function:

$$R_k = e^{-\theta_k \left| x_k^{(i)} - x_k^{(j)} \right|^2}. \tag{18}$$

- "CUBIC SPLINE" correlation function:

$$R_k = \begin{cases} 1 - 15\xi_k^2 + 30\xi_k^3 & \text{for } 0 \leqslant \xi_k \leqslant 0.2, \\ 1.25(1 - \xi_k)^3 & \text{for } 0.2 < \xi_k < 1, \\ 0 & \text{for } \xi_k \geqslant 1, \end{cases}$$

$$\text{where } \xi_k = \theta_k \left| x_k^{(i)} - x_k^{(j)} \right|. \tag{19}$$

Taking the GAUSS correlation function as an example, its 1st- and 2nd-order partial derivatives are of the form:

$$\frac{\partial R(\mathbf{x}^{(i)}, \mathbf{x}^{(j)})}{\partial x_k^{(i)}} = -2\theta_k \big(x_k^{(i)} - x_k^{(j)}\big) R\big(\mathbf{x}^{(i)}, \mathbf{x}^{(j)}\big),$$

$$\frac{\partial R(\mathbf{x}^{(i)},\mathbf{x}^{(j)})}{\partial x_k^{(j)}} = 2\theta_k\big(x_k^{(i)} - x_k^{(j)}\big)R\big(\mathbf{x}^{(i)},\mathbf{x}^{(j)}\big),$$

$$\frac{\partial^2 R(\mathbf{x}^{(i)},\mathbf{x}^{(j)})}{\partial x_l^{(i)}\partial x_k^{(j)}} = \begin{cases} 2\theta_k[-2\theta_k(x_k^{(i)} - x_k^{(j)})^2 + 1.0]R(\mathbf{x}^{(i)},\mathbf{x}^{(j)}), & k = l, \\ -4\theta_k\theta_l(x_k^{(i)} - x_k^{(j)})(x_l^{(i)} - x_l^{(j)})R(\mathbf{x}^{(i)},\mathbf{x}^{(j)}), & k \neq l. \end{cases} \tag{20}$$

3.3. Model fitting by Maximum Likelihood Estimation (MLE)

Given a set of data assumed to be distributed according to some mathematical model, Maximum Likelihood Estimation (MLE) is concerned with fitting the model to the data by tuning its free hyper-parameters. More precisely, the MLE of the model is obtained by maximizing the probability density function (PDF) associated to the random process at hand with respect to the expectation values and the co-variances.

In the above setting, the expectation is given by β_0 (see Eq. (4)) and the co-variances are functions of the process variance σ^2 and the distance weights $\boldsymbol{\theta} = (\theta_1, \ldots, \theta_m)$, which parameterize the correlation model, see Section 3.2. Optimal estimations of the mean

$$\beta_0(\boldsymbol{\theta}) = \big(\mathbf{F}^{\mathrm{T}}\mathbf{R}^{-1}\mathbf{F}\big)^{-1}\mathbf{F}^{\mathrm{T}}\mathbf{R}^{-1}\mathbf{y}_{\mathrm{S}} \tag{21}$$

and the process variance

$$\sigma^2(\boldsymbol{\theta}) = \frac{1}{n+n'}(\mathbf{y}_{\mathrm{S}} - \beta_0\mathbf{F})^{\mathrm{T}}\mathbf{R}^{-1}(\mathbf{y}_{\mathrm{S}} - \beta_0\mathbf{F}) \tag{22}$$

are obtained analytically, yet depend on the remaining hyper-parameters $\boldsymbol{\theta} = (\theta_1, \ldots, \theta_m)$. Substituting these values in the associated PDF and taking the logarithm, we are left with maximizing

$$\mathrm{MLE}(\boldsymbol{\theta}) = -\big(n+n'\big)\ln\sigma^2(\boldsymbol{\theta}) - \ln\big[\det\mathbf{R}(\boldsymbol{\theta})\big]. \tag{23}$$

Following the approach presented in Ref. [24], we solve this optimization problem approximately by using a modified version of the Direct Search algorithm of Hooke and Jeeves [25]. Given initial parameters $\boldsymbol{\theta}_{\mathrm{init}}$, this method consists of two steps:

(1) *Explore* the local behavior of the objective function by comparing function values at points which are a certain step size away from $\boldsymbol{\theta}_{\mathrm{init}}$ to arrive at a new base point $\boldsymbol{\theta}'$. Store the direction in which an improvement of the objective function was obtained.
(2) *Move* along this direction to a next base point as long as the value of the objective function increases.

To keep computational costs at a manageable size, these two steps are repeated a fixed number of times, depending on the problem dimension, for details, see [24]. As with any local optimization method, the algorithm is sensitive to the choice of the starting point.

3.4. Remarks on the difference between GEK and cokriging

Cokriging was firstly developed in the geostatistics community [26] for the prediction of an under-sampled primary variable of interest by better sampled auxiliary variables. Cokriging was extended to variable-fidelity surrogate modeling problems (see [2,27, 28]). As the idea of GEK is very similar to two-variable cokriging, Chung and Alonso called their GEK method "cokriging" in Ref. [16] and Ref. [17], taking the function as the primary variable and the gradient as the auxiliary variable. In their terminology, the direct way to implement GEK is called "direct cokriging" and the indirect way is called "indirect cokriging". However, in our opinion, GEK is actually not a two-variable cokriging method as there are some distinct differences between the two. The differences are listed as follows:

(1) The unbiasedness condition is different. For two-variable ordinary cokriging, the unbiasedness condition requires that the sum of the weight coefficients for primary variable equals "1" and that the sum of the weight coefficients for auxiliary variable equals to "0". The unbiasedness condition for ordinary GEK is that the sum of the weight coefficients for the primary function values is equal to "1". If one also sets the sum of weight coefficients for the partial derivatives to "0", a mistake is caused. For example, if only one partial derivative is considered at only one sample site, the corresponding weight coefficient would have to be "0" to fulfill the unbiasedness condition, and, as a consequence, the gradient would have no effect on the prediction. It is known, however, that the prediction can still be improved even if only one partial derivative is enforced at a single sample site.
(2) The "isotopic condition" does not hold for GEK. For two-variable cokriging, it is well known that there will be no improvement if the auxiliary variable is sampled at the same site as the primary variable (called isotopic condition). However, for GEK, the prediction can be improved if the gradient information is obtained at the location of the sample point for the primary function [16,17], which is essentially the whole idea of GEK.
(3) The number of auxiliary variables is different. From the point of view of cokriging, there will be m auxiliary variables if the gradients w.r.t. m independent variables are used. In other words, the number of auxiliary variable is not "1" but m. Therefore, it makes no sense to construct GEK models using the same way as cokriging models with two variables.

From the above remarks, we conclude that the term "GEK" is more appropriate than "cokriging".

4. A generalized hybrid bridge function

One of the key issues for VFM is how to manage the different models of varying fidelity or how to correct the low-fidelity model to approximate the high-fidelity data by making use of so-called "bridge functions", which are sometimes called "scaling functions". The existing bridge functions can be divided into three categories:

- Multiplicative (see Refs. [3–6]),
- Additive (see Refs. [7–10]),
- Hybrid (see Refs. [11–13]).

All these approaches require the construction of an unknown function to correct the lower-fidelity model, which in turn will approximate the high-fidelity model. Note that the bridge functions can take the form of low-order polynomials or kriging models. They can also take the form of a GEK model (see Section 3). A detailed description of different bridge function methods can be found in [29].

4.1. Multiplicative bridge function

The multiplicative bridge function can be defined as

$$\phi(\mathbf{x}) = \frac{y_{\mathrm{hf}}(\mathbf{x})}{y_{\mathrm{lf}}(\mathbf{x})}, \tag{24}$$

where $y_{\mathrm{lf}}(\mathbf{x})$ and $y_{\mathrm{hf}}(\mathbf{x})$ denote the low- and high-fidelity models, respectively. After the exact but unknown bridge function $\phi(\mathbf{x})$ and low-fidelity model $y_{\mathrm{lf}}(\mathbf{x})$ have been approximated with $\hat{\phi}(\mathbf{x})$

and $\hat{y}_{\mathrm{lf}}(\mathbf{x})$, respectively, the high-fidelity model $y_{\mathrm{hf}}(\mathbf{x})$ can be approximated by the VFM as

$$\hat{y}_{\mathrm{hf}}(\mathbf{x}) = \hat{\phi}(\mathbf{x})\hat{y}_{\mathrm{lf}}(\mathbf{x}). \tag{25}$$

It can be shown that the function $\phi(\mathbf{x})$ is the scaling ratio between the high-fidelity data and the low-fidelity model, and when it is multiplied by the low-fidelity model, the response of the high-fidelity model is achieved. However, the above multiplicative bridge function may cause problems when one of the sampled values of the low-fidelity model is close to zero.

4.2. Additive bridge function

To avoid the possible problem of dividing by zero when using multiplicative bride functions, an additive bridge function was developed by Lewis and Nash [7]. The additive bridge function can be expressed as

$$\gamma(\mathbf{x}) = y_{\mathrm{hf}}(\mathbf{x}) - y_{\mathrm{lf}}(\mathbf{x}), \tag{26}$$

where $y_{\mathrm{lf}}(\mathbf{x})$ and $y_{\mathrm{hf}}(\mathbf{x})$ denote the low- and high-fidelity models, respectively. After the exact but unknown bridge function $\gamma(\mathbf{x})$ and low-fidelity model $y_{\mathrm{lf}}(\mathbf{x})$ have been approximated with $\hat{\gamma}(\mathbf{x})$ and $\hat{y}_{\mathrm{lf}}(\mathbf{x})$, respectively, the high-fidelity model $y_{\mathrm{hf}}(\mathbf{x})$ can be approximated by the VFM as

$$\hat{y}_{\mathrm{hf}}(\mathbf{x}) = \hat{y}_{\mathrm{lf}}(\mathbf{x}) + \hat{\gamma}(\mathbf{x}). \tag{27}$$

It can be shown that the function $\gamma(\mathbf{x})$ is essentially the error or difference between the low- and high-fidelity models. When $\hat{\gamma}(\mathbf{x})$ is added to the low-fidelity model, the response of the high-fidelity model is obtained.

4.3. Adaptive hybrid bridge functions

Gano et al. [11,12] showed that additive bridge functions are not always better than multiplicative ones. Both have merits and demerits. Hence, Gano et al. developed an adaptive hybrid method that combines the multiplicative and additive methods

$$\hat{y}(\mathbf{x}) = \omega \cdot \hat{\phi}(\mathbf{x})\hat{y}_{\mathrm{lf}}(\mathbf{x}) + (1-\omega)\cdot\left[\hat{y}_{\mathrm{lf}}(\mathbf{x}) + \hat{\gamma}(\mathbf{x})\right], \tag{28}$$

where ω is a weight coefficient. The determination of ω may be the key point for the success of this hybrid bridge function. Eldred et al. [13] proposed to use the previously evaluated point to adjust the value of ω:

$$\omega = \frac{y_{\mathrm{hf}}(\mathbf{x}_{\mathrm{old}}) - [\hat{y}_{\mathrm{lf}}(\mathbf{x}_{\mathrm{new}}) + \hat{\gamma}(\mathbf{x}_{\mathrm{new}})]}{\hat{\phi}(\mathbf{x}_{\mathrm{new}})\hat{y}_{\mathrm{lf}}(\mathbf{x}_{\mathrm{new}}) - [\hat{y}_{\mathrm{lf}}(\mathbf{x}_{\mathrm{new}}) + \hat{\gamma}(\mathbf{x}_{\mathrm{new}})]}, \tag{29}$$

where $y_{\mathrm{hf}}(\mathbf{x}_{old})$ denotes the optimum of the previous optimization step. During the process of optimization, a new value can be computed at each iteration. Updating these weights allows the framework to adapt to the best model for the region near the optimum in the design space.

Note that the above adaptive hybrid bridge function is designed particularly in the optimization context. The problem becomes quite different for the construction of a VFM for aero-loads prediction, where a global model in a relatively large parameter space is sought after. The authors' experience suggests that the above approach developed in the optimization context does not work because the old value $y_{\mathrm{hf}}(\mathbf{x}_{old})$ is not available. Therefore, we need to use a more general way for the construction of hybrid bridge function.

4.4. Generalized hybrid bridge function

In this article, a new method for constructing a hybrid bridge function in the context of global surrogate modeling of an unknown aerodynamic function based on sampled data from numerical methods of different degrees of fidelity is proposed. In a first step, a low-order polynomial (called RSM in the text below) is used to describe the appropriate multiplicative scaling between the high- and low-fidelity models (called RSM-type "multiplicative" bridge function). In a second step, a kriging model is used to describe the difference between the high-fidelity model and the scaled low-fidelity model (called kriging-type "additive" bridge function, which is used to correct the kriging model for the low-fidelity data to better approximate the high fidelity data). The new hybrid bridge function is motivated by the following thinking:

(1) The key idea of VFM is to map the trend of the unknown function underlying the intensively sampled low-fidelity data to the less intensively sampled high-fidelity data by a so-called "bridge function".
(2) The relationship between the low- and high-fidelity data can be described by two kinds of functions: multiplicative and additive. The multiplicative bridge function is a low-order polynomial (constant, linear or second order RSM). The additive bridge function should also be of low order but of higher order than the multiplicative one. In a realistic problem, both relationships can exist.
(3) In general, additive bridge functions are more accurate and robust than multiplicative bridge functions. However, they are not always better than multiplicative ones. In some cases, multiplicative bridge functions may perform better.
(4) As the multiplicative bridge function is assumed to be of low-order, a low-order RSM can be used to represent it. The advantage of using an RSM-type multiplicative bridge function is that its hyper-parameters can be optimized subordinated to the maximum likelihood fitting of the kriging model for the additive bridge function. Therefore, a close relationship between both types of bridge functions is established by taking model training aspects into account.
(5) Traditional hybrid bridge functions [11–13] use a weighted sum of multiplicative and additive bridge functions. This method is not suitable for VFM in the context of aero-loads prediction. We feel that the benefit of including the low-fidelity model can be further exploited by using the hybrid bridge function in a more general way.

Based on the above reasoning as well as our experience working on VFM, a Generalized Hybrid Bridge Function (GHBF) is developed to fully exploit the trend underlying the low-fidelity data, which is used to assist the prediction of the high-fidelity function. Note that this new bridge function is designed to fulfill the following basic conditions:

(1) *Interpolation condition*: The high-fidelity sampled data should be exactly reproduced, as there is no random error existing for a deterministic computer experiment.
(2) *Convergence condition*: With an increasing number of high-fidelity samples, the influence of the low-fidelity data on the VFM should be gradually decreased, that is, the VFM should converge to the exact functional relationship.

For an m-dimensional problem, assume that we have sampled the low-fidelity model at n_{lf} points and the high-fidelity model at n_{hf} points (assume $n_{\mathrm{lf}} \gg n_{\mathrm{hf}}$) with

$$\mathbf{S}_{\mathrm{lf}} = \left(\mathbf{x}_{\mathrm{lf}}^{(1)}, \ldots, \mathbf{x}_{\mathrm{lf}}^{(n_{\mathrm{lf}})}\right)^{\mathrm{T}} \in \mathbb{R}^{n_{\mathrm{lf}} \times m},$$

$$\mathbf{y}_{S,lf} = \left(y_{lf}^{(1)}, \ldots, y_{lf}^{(n_{lf})}\right)^T \in \mathbb{R}^{n_{lf}},$$
$$\mathbf{S}_{hf} = \left(\mathbf{x}_{hf}^{(1)}, \ldots, \mathbf{x}_{hf}^{(n_{hf})}\right)^T \in \mathbb{R}^{n_{hf} \times m},$$
$$\mathbf{y}_{S,hf} = \left(y_{hf}^{(1)}, \ldots, y_{hf}^{(n_{hf})}\right)^T \in \mathbb{R}^{n_{hf}}. \quad (30)$$

Enforcing the above conditions, the VFM algorithm with a GHBF is developed as described in the following. First, we express the relationship between the low- and high-fidelity models as

$$y_{hf}(\mathbf{x}) = \phi(\mathbf{x}) \cdot y_{lf}(\mathbf{x}) + \gamma(\mathbf{x}), \quad (31)$$

where $\gamma(\mathbf{x})$ is the bridge function, $\phi(\mathbf{x}) = \mathbf{f}_\phi^T(\mathbf{x})\boldsymbol{\rho}$ is a low-order polynomial (RSM) with $\mathbf{f}_\phi(\mathbf{x}) = [1, f_1(\mathbf{x}), \ldots, f_q(\mathbf{x})]^T$ being $q+1$ basis functions and $\boldsymbol{\rho} = (\rho_0, \rho_1, \ldots, \rho_q)^T$ being the corresponding coefficients (e.g. $q=0$ is for constant regression and $q=m$ for linear regression). Note that an expression of the form of Eq. (31) always exists. Next, we take $y_{lf}(\mathbf{x})$ and $\gamma(\mathbf{x})$ as random functions and try to create kriging models for them; the vector $\boldsymbol{\rho}$ is estimated when fitting the kriging model for $\gamma(\mathbf{x})$ using MLE. The building of the VFM with the idea of this hybrid function can be achieved by the following three steps:

(1) *Kriging model for low-fidelity data*: Based on the low-fidelity sample data set $(\mathbf{S}_{lf}, \mathbf{y}_{S,lf})$ only, a kriging predictor is built as

$$\hat{y}_{lf}(\mathbf{x}) = \mathbf{f}_{lf}^T(\mathbf{x})\boldsymbol{\beta}_{lf} + \mathbf{r}^T(\mathbf{x})\mathbf{R}^{-1}(\mathbf{y}_{S,lf} - \mathbf{F}\boldsymbol{\beta}_{lf}), \quad (32)$$

where $\mathbf{r} \in \mathbb{R}^{n_{lf}}, \mathbf{R} \in \mathbb{R}^{n_{lf} \times n_{lf}}$ are the correlation vector and correlation matrix, respectively, $\mathbf{f}_{lf}(\mathbf{x})$ and $\mathbf{F}$ are the basis functions and the corresponding regression matrix for the kriging model, respectively, and $\boldsymbol{\beta}_{lf} = (\mathbf{F}^T\mathbf{R}^{-1}\mathbf{F})^{-1}\mathbf{F}^T\mathbf{R}^{-1}\mathbf{y}_{S,lf}$ is the usual MLE of the regression coefficient vector. The reader is also referred to Ref. [23] for the details on the kriging predictor and hyper parameter estimation.

(3) *Kriging model for the bridge function:* The sampled data for the bridge function, $\boldsymbol{\gamma}_S = (\gamma^{(1)}, \ldots, \gamma^{(n_{hf})})^T$, can then be found by

$$\gamma^{(i)} := y\left(\mathbf{x}_{hf}^{(i)}\right) - \sum_{j=0}^{q} \hat{y}_{lf}\left(\mathbf{x}_{hf}^{(i)}\right) f_j\left(\mathbf{x}_{hf}^{(i)}\right)\rho_j, \quad i = 1, \ldots, n_{hf} \quad (33)$$

or, in matrix form,

$$\boldsymbol{\gamma}_S = \mathbf{y}_{S,hf} - \boldsymbol{\Gamma}\boldsymbol{\rho},$$

where

$$\boldsymbol{\Gamma} \in \mathbb{R}^{n_{hf} \times (q+1)} \quad \text{with } \Gamma_{ij} = \hat{y}_{lf}\left(\mathbf{x}_{hf}^{(i)}\right) f_j\left(\mathbf{x}_{hf}^{(i)}\right),$$
$$i = 1, \ldots, n_{hf},\ j = 0, \ldots, q. \quad (34)$$

Note that $\hat{y}_{lf}(\mathbf{x}_{hf}^{(i)})$ is the kriging approximation of the low-fidelity model at the sample sites of the high-fidelity model. Based on the sampled data set for the bridge function (sample sites are the same as for the high-fidelity model), the kriging predictor of $\gamma(\mathbf{x})$ can be built as

$$\hat{\gamma}(\mathbf{x}) = \mathbf{f}_\gamma^T(\mathbf{x})\boldsymbol{\beta}_\gamma + \tilde{\mathbf{r}}^T(\mathbf{x})\tilde{\mathbf{R}}^{-1}[\boldsymbol{\gamma}_S - \tilde{\mathbf{F}}\boldsymbol{\beta}_\gamma], \quad (35)$$

where symbols $\tilde{\mathbf{r}} \in \mathbb{R}^{n_{hf}}, \tilde{\mathbf{R}} \in \mathbb{R}^{n_{hf} \times n_{hf}}$ denote the correlation vector and correlation matrix, respectively, $\mathbf{f}_\gamma(\mathbf{x})$ and $\tilde{\mathbf{F}}$ are the basis functions and the corresponding regression matrix for the kriging model, respectively, and $\boldsymbol{\beta}_\gamma = (\tilde{\mathbf{F}}^T\tilde{\mathbf{R}}^{-1}\tilde{\mathbf{F}})^{-1}\tilde{\mathbf{F}}^T\tilde{\mathbf{R}}^{-1}\boldsymbol{\gamma}_S$ is the usual MLE of the associated regression coefficient vector. The construction of $\hat{\gamma}(\mathbf{x})$ is similar to that described in Ref. [23] but with additional parameters $\boldsymbol{\rho} = (\rho_0, \rho_1, \ldots, \rho_q)^T$ to be estimated. Differentiating the associated maximum likelihood function shows that the optimal coefficient vector $\boldsymbol{\rho}$ depends on the remaining parameters and is given by

$$\boldsymbol{\rho} = \left(\boldsymbol{\Gamma}^T\tilde{\mathbf{R}}^{-1}\boldsymbol{\Gamma}\right)^{-1}\boldsymbol{\Gamma}^T\tilde{\mathbf{R}}^{-1}(\mathbf{y}_{S,hf} - \tilde{\mathbf{F}}\boldsymbol{\beta}_\gamma). \quad (36)$$

The initial value of $\boldsymbol{\rho}$ can be taken as $(1, 0, \ldots, 0)^T$. Then it is updated at each iteration of the MLE.

(4) *VFM approximation of the high-fidelity model*: Once $\hat{y}_{lf}(\mathbf{x})$, $\hat{\gamma}(\mathbf{x})$, $\phi(\mathbf{x}) = \mathbf{f}_\phi^T(\mathbf{x})\boldsymbol{\rho}$ are constructed, the VFM approximation of the high-fidelity model can be obtained by

$$\hat{y}_{hf}(\mathbf{x}) = \mathbf{f}_\phi^T(\mathbf{x})\boldsymbol{\rho} \cdot \hat{y}_{lf}(\mathbf{x}) + \hat{\gamma}(\mathbf{x}). \quad (37)$$

Assuming that the random processes corresponding to $y_{lf}(\mathbf{x})$ and $\gamma(\mathbf{x})$ are unbiased and independent from each other, the MSE of this VFM prediction is given by

$$\mathrm{MSE}\left[\hat{y}_{hf}(\mathbf{x})\right] = \left[\mathbf{f}_\phi^T(\mathbf{x})\boldsymbol{\rho}\right]^2 \cdot \mathrm{MSE}\left[\hat{y}_{lf}(\mathbf{x})\right] + \mathrm{MSE}\left[\hat{\gamma}(\mathbf{x})\right], \quad (38)$$

where $\mathrm{MSE}[\hat{y}_{lf}(\mathbf{x})]$ and $\mathrm{MSE}[\hat{\gamma}(\mathbf{x})]$ are the kriging mean squared error for the low-fidelity model $y_{lf}(\mathbf{x})$ and the bridge function $\gamma(\mathbf{x})$, respectively.

Note that different sets of basis functions may be chosen for $\mathbf{f}_\phi(\mathbf{x})$, $\mathbf{f}_{lf}(\mathbf{x})$, $\mathbf{f}_\gamma(\mathbf{x})$. The method described above is classified as a VFM with a generalized hybrid bridge function as it is not only the combination of multiplicative and additive bridge functions but also the combination of RSM-based and kriging-based bridge functions. It is a generalization of multiplicative and additive bridge functions and offers the advantages of both types of bridge functions and those of both meta-modeling methods. This method is verified and demonstrated in Section 5. Please also note that gradient information can be exploited in order to improve the accuracy of the GHBF, which results in a method that we will call gradient-enhanced GHBF.

5. Numerical examples

5.1. Examples for the direct GEK method

The direct GEK method outlined above was implemented into a C-language toolbox. The functionality of the code was designed to integrate the codes for kriging, indirect GEK and direct GEK into a single code, which makes it very practical to use. The direct GEK code is fully verified by constructing an approximation model for analytical functions based on sampled data in [29]. Here, the surrogate model for the aerodynamic coefficient of an RAE 2822 airfoil are constructed to demonstrate the applicability of the direct GEK method with the gradients computed by adjoint method [30]. Subsequently, the direct GEK is used to construct a VFM model for an analytical problem based on a gradient-enhanced bridge function. It is shown that the use of direct GEK in constructing a VFM model leads to a more efficient and accurate method.

5.1.1. Direct GEK with gradients computed via the adjoint method

The benefit of using GEK is that the gradient information for a high-dimensional problem can be efficiently computed using the adjoint approach [30]. The advantage of the adjoint formulation is that it enables the computation of sensitivity derivatives of a given objective function or output functional at a cost which is essentially independent of the number of design variables, requiring only a single flow solution and a single adjoint solution for any number of design variables [31]. Here, the use of the adjoint formulation to efficiently obtain the gradients needed by GEK to improve the accuracy of the approximation is the core idea.

The use of GEK with the adjoint method was demonstrated for modeling the aerodynamic coefficients and drag polar of an RAE 2822 airfoil at a Mach number of 0.73 based on Euler computations. The TAU Euler solver (see Refs. [32–35]) and the discrete TAU adjoint Euler solver (see Refs. [36–38]) were used for

the flow simulations and for computing the gradient information, respectively. The computational grid is shown in Fig. 2. Both the flow solver and the discrete adjoint solver use Jameson's central scheme. Results for the drag coefficient versus angle of attack are shown in Fig. 3. Seven samples in the range $-12^\circ \leqslant \alpha \leqslant +12^\circ$ were used to construct the direct GEK model. Both the drag coefficient and the gradient of the drag coefficient with respect to the angle of attack were considered at all sample sites. Euler computations were also performed at a total of 35 sample sites to obtain validation data (red square symbols) for verifying the direct GEK method as well as the code. It is observed in Fig. 3 that the accuracy of the approximation model is significantly improved by using the direct GEK method. This example is a preliminary demonstration of direct GEK combined with the adjoint method. Note that the main benefit of GEK – improved accuracy due to gradient information at a cost which is essentially independent of the number of design variables – does not come into effect until multi-dimensional problem are considered, for which the adjoint method is much more efficient than the traditional finite-difference method.

5.1.2. Preliminary demonstration of GEK for VFM

As discussed before, the incorporation of the gradient information in GEK provides a very promising strategy that can be used to significantly improve the accuracy of kriging for a given number of samples. In turn, the efficiency of constructing an approximation model for an unknown aerodynamic function can be improved as fewer samples are needed for a given level of accuracy, especially for high-dimensional problems. For VFM, the incorporation of lower-fidelity data also provides a promising way to improve the accuracy or efficiency. Our idea is that GEK will lead to a VFM method that is more efficient and accurate. For a start, this idea is demonstrated for an analytic problem taken from [21]. The analytical function $y_{\mathrm{hf}} = (6x-2)^2 \sin(12x-4), x \in [0,1]$, represents the high-fidelity model and the low-fidelity model is given by $y_{\mathrm{lf}} = 0.5y_{\mathrm{hf}} + 10(x-0.5) - 5$. The x-locations of the low and high-fidelity samples are $\mathbf{S}_{\mathrm{lf}} = \{0.0, 0.1, 0.2, 0.3, 0.4, 0.5, 0.6, 0.7, 0.8, 0.9, 1.0\}$ and $\mathbf{S}_{\mathrm{hf}} = \{0.0, 0.4, 0.6, 1\}$, respectively. Rather than using GEK to improve the kriging approximation of the low- or high-fidelity data, it was used to improve the kriging model of the "additive" bridge function, assuming that the gradient of y_{hf} is available at each sample site $\mathbf{S}_{\mathrm{hf}}$. Note that the gradient of the bridge function is defined as $\partial(y_{\mathrm{hf}} - y_{\mathrm{lf}})/\partial x = \partial y_{\mathrm{hf}}/\partial x - \partial y_{\mathrm{lf}}/\partial x$ and was sampled at $\mathbf{S}_{\mathrm{hf}}$. As we assume that a large number of low-fidelity samples are available, $\partial y_{\mathrm{lf}}/\partial x$ can be estimated based on the sampled data using the "kriging gradient predictor" according to Eq. (15) (predict the gradient of the unknown function based on its kriging approximation), while $\partial y_{\mathrm{lf}}/\partial x$ needs to be sampled. The correlation coefficients $\boldsymbol{\theta}$ of the GAUSS correlation function is optimized for both the kriging and the GEK model using MLE. The results are shown in Fig. 4. The VFM with a kriging-based bridge function (black dash-dotted line) and the VFM with a GEK-based bridge function (green solid line) are compared with the exact function (red square symbols). The result for kriging (blue dash-dotted line) using only the four high-fidelity samples (blue square symbols) is also plotted in Fig. 4. This comparison shows that the VFM with a GEK-based bridge function is more accurate. The gradients at

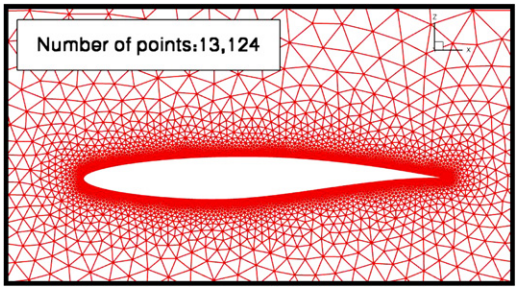

Fig. 2. Unstructured grid for the RAE 2822 airfoil used for inviscid flow computations.

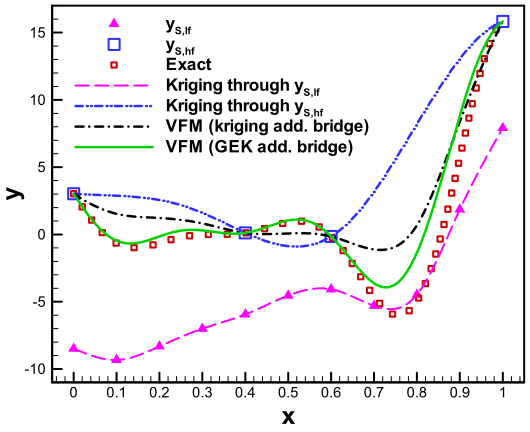

Fig. 4. Comparison of VFM models using the kriging and GEK-based additive bridge functions with kriging of high-fidelity samples and the exact analytical function. (For interpretation of the references to color in this figure, the reader is referred to the web version of this article.)

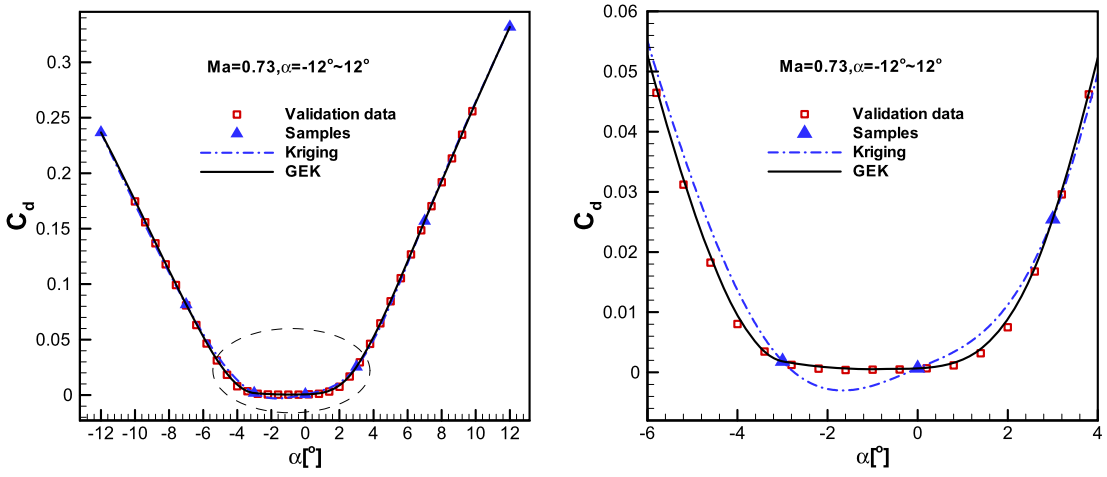

Fig. 3. Direct GEK for the drag coefficient of the RAE 2822 airfoil compared to kriging and validation data ($Ma = 0.73, \alpha \in [-12^\circ, +12^\circ]$, left: overall view; right: detailed view).

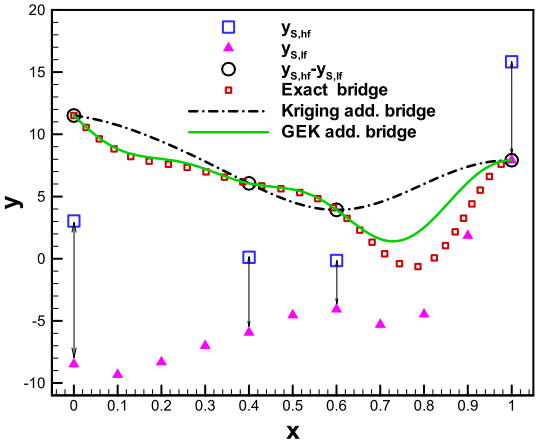

Fig. 5. Comparison of the exact bridge function with the kriging- and GEK-based additive bridge functions. (For interpretation of the references to color in this figure, the reader is referred to the web version of this article.)

the samples are correctly reproduced. The reason can be found in Fig. 5 in which the kriging-based bridge function (black dash-dotted line) and GEK-based bridge function (green solid line) are compared with the exact bridge function (red square symbols), $y_{hf} - y_{lf}$. It is evident that the GEK-based bridge function is much better than kriging-based bridge function, which leads to a more accurate VFM.

5.2. Examples for the use of the GHBF method

The use of the GHBF method, which was derived in Section 4.4, is demonstrated for an analytical problem as well as for constructing a VFM model of the aerodynamic coefficients and the drag polar of an RAE 2822 airfoil.

5.2.1. Verification of the GHBF-based VFM for an analytical problem

The same analytical problem as used in Fig. 4 and Fig. 5 is employed here to compare the GHBF (see Section 4) with the additive bridge without any gradient information. The results are shown in Fig. 6 (left). The VFM based on the GHBF method (green solid line) shown in Fig. 6 is in very good agreement with the exact function (red square symbols), which shows the feasibility and correctness of the proposed GHBF method. Note that both constant regression ($q = 0$) and linear regression ($q = m$) were used for the scaling function $\phi(\mathbf{x})$. The hyper parameters of the GAUSS correlation function, including the correlation coefficient vector $\boldsymbol{\theta}$, were optimized by MLE. After hyper-parameter optimization, the MLEs of ρ for constant and linear scaling were found to be 2.0 and (2.0, 0.0), respectively, which is consistent with true functional relationship between the low- and high-fidelity models. With these scaling factors, the exact bridge function is $y_{hf} - 2.0y_{lf} = -20(x - 0.5) + 10$ (a linear function). Hence, a kriging model with four samples can accurately approximate this linear function, which is a good explanation for why we can get a nearly perfect agreement between the VFM model with the GHBF and the exact function in Fig. 6. However, in the case of the additive bridge function, the exact bridge function, $y_{hf} - y_{lf} = 0.5(6x - 2)^2 \sin(12x - 4) - 10(x - 0.5) + 5$, is a highly non-linear function, which cannot be approximated well by only using four samples (see Fig. 6). The comparison of the root mean squared error is also displayed in Fig. 6 (right), which demonstrates that the GHBF results in much smaller mean squared error and thus a more accurate VFM model.

To show the difference between constant scaling ($q = 0$) and linear scaling ($q = m$), the analytical example is slightly modified. The high-fidelity function and the sample sites are the same as in Fig. 6, but the low-fidelity function is changed to $y_{lf} = [y_{hf} + 10(x - 0.5) - 5]/(1.0 + 1.5x)$. The comparison of the VFM models with constant- and linear scaling for the GHBFs ($q = 0$ and $q = m$, respectively) are shown in Fig. 7 (left). It can be observed that linear scaling is better than constant scaling as the exact scaling function between the high- and low-fidelity models is linear. The corresponding root mean squared error is also shown in Fig. 7 (right), which demonstrates that a GHBF with constant scaling gives larger uncertainty than one with linear scaling, but smaller uncertainty than an additive bridge function.

5.2.2. Demonstration of GHBF-based VFM for RAE 2822 airfoil

Next, we consider again the RAE 2822 airfoil and use the GHBF method to generate VFM models for the aerodynamic coefficients as a function of only one independent variable, α. The Mach number and the Reynolds number were taken as 0.2 and 6.5×10^6, respectively. The angle of attack, α, varied between $-4°$ and $+16.5°$. The computational grids for Euler and Navier–Stokes computations with the DLR TAU code (see Refs. [32–35]) are shown in Fig. 8.

The VFM models with the GHBF for the different aerodynamic coefficients are shown in Fig. 9, where the results for lift vs. angle of attack and drag vs. angle of attack and the corresponding drag polar are displayed. The VFM models (black solid line) are based on 26 low- and as few as 3 high-fidelity samples. They are compared with kriging of the three high-fidelity samples (blue dash-dotted

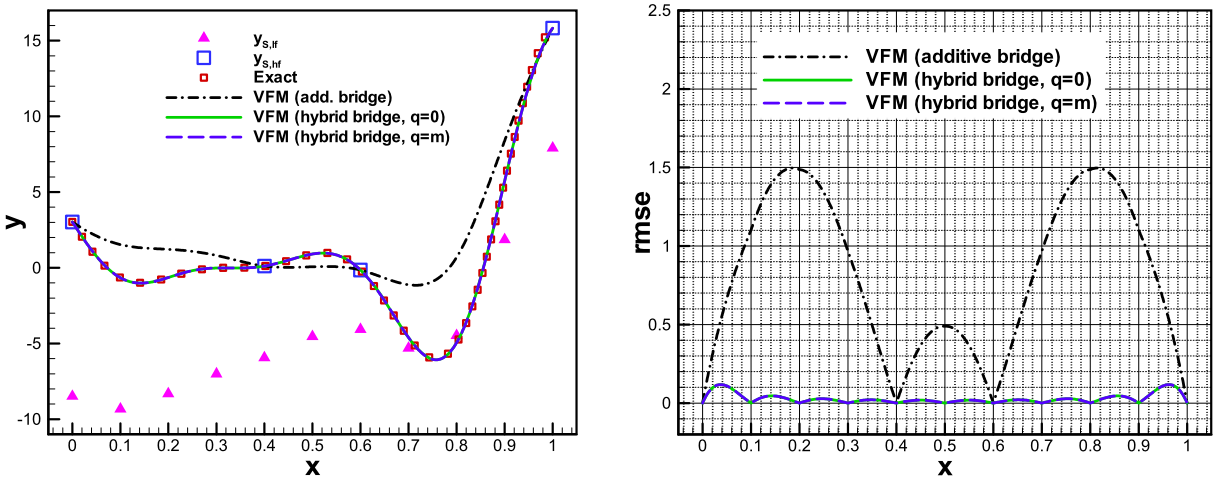

Fig. 6. Comparison of VFMs with additive and generalized hybrid bridge functions (left: function value, right: root mean squared error). (For interpretation of the references to color in this figure, the reader is referred to the web version of this article.)

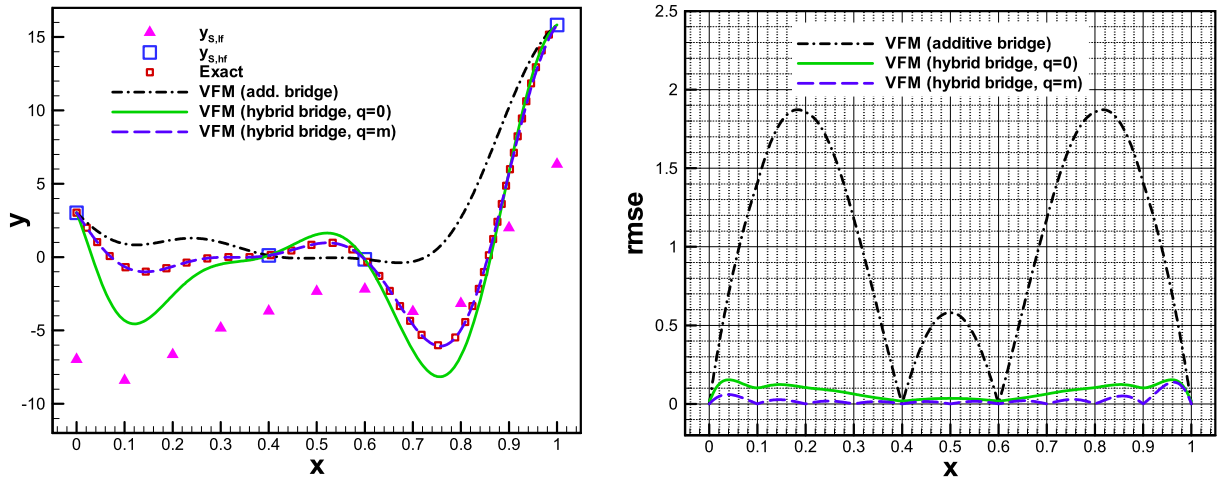

Fig. 7. Comparison of VFMs with constant and linear-scaling functions used to construct the hybrid bridge functions (left: function value, right: root mean squared error).

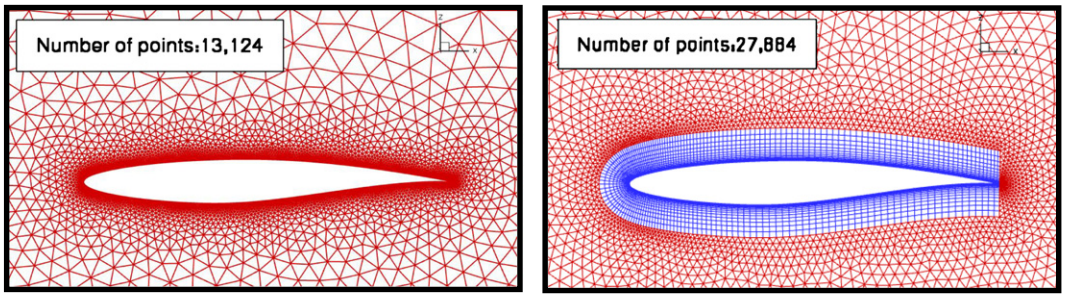

Fig. 8. Numerical grids for the low- and high-fidelity computations of the flow around the RAE 2822 airfoil.

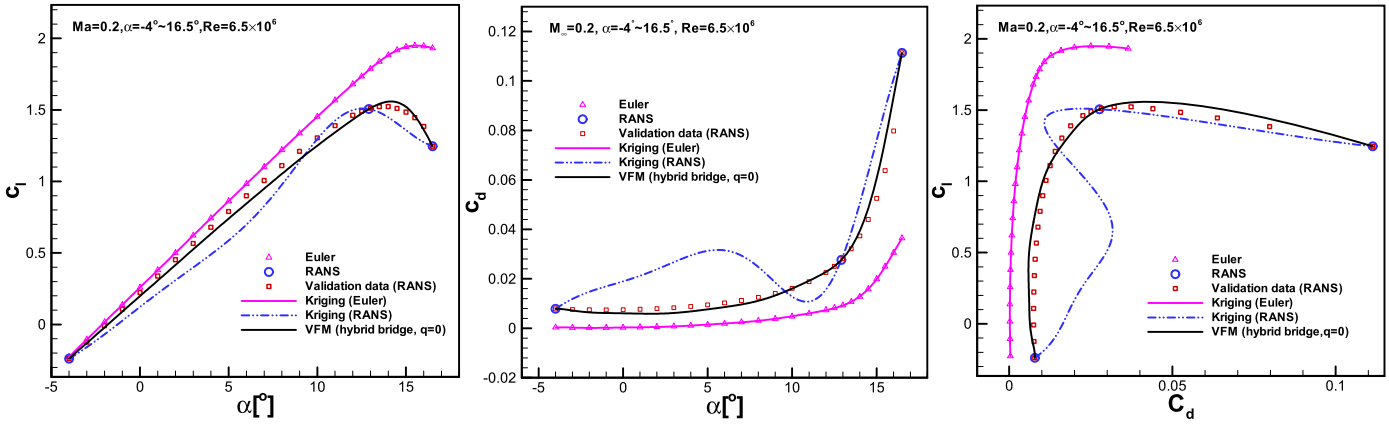

Fig. 9. VFM for the lift coefficient (left), drag coefficient (middle) and the drag polar (right) for the RAE 2822 airfoil based on the Generalized Hybrid Bridge Function (GHBF). (For interpretation of the references to color in this figure, the reader is referred to the web version of this article.)

line) and validation data (red square symbols). The comparison shows that VFM with the GHBF is very promising for constructing a global approximation model for aerodynamic data. Note that in this example, little differences can be found between the GHBF-based VFM models with constant ($q = 0$) and linear ($q = m$) scaling, and only the results via constant scaling is shown in Fig. 9.

The GHBF (black solid line) was also compared with the traditional additive (red dash-dotted line) and multiplicative (green dash-dotted line) bridge functions, as shown in Fig. 10 for the same test case. Fig. 10 shows the VFM models for the lift and drag coefficient versus angle of attack and the drag polar. The VFM models based on the additive and multiplicative bridge functions show significant discrepancy to the validation data (red square symbols) over the entire angle-of-attack range, while the VFM based on the GHBF is in much better agreement with the validation data. The VFM based on the multiplicative bridge function is slightly better than that based on the additive bridge function in terms of its behavior in the linear range, which confirms that additive bridge functions are not always better than multiplicative ones. The VFM based on the GHBF is in best agreement with the validation data. Small discrepancies to the validation data are observed around the stall angle. Both the additive and the multiplicative bridge function-based VFM models exhibit oscillations, which are not present in the validation data, while the GHBF-based

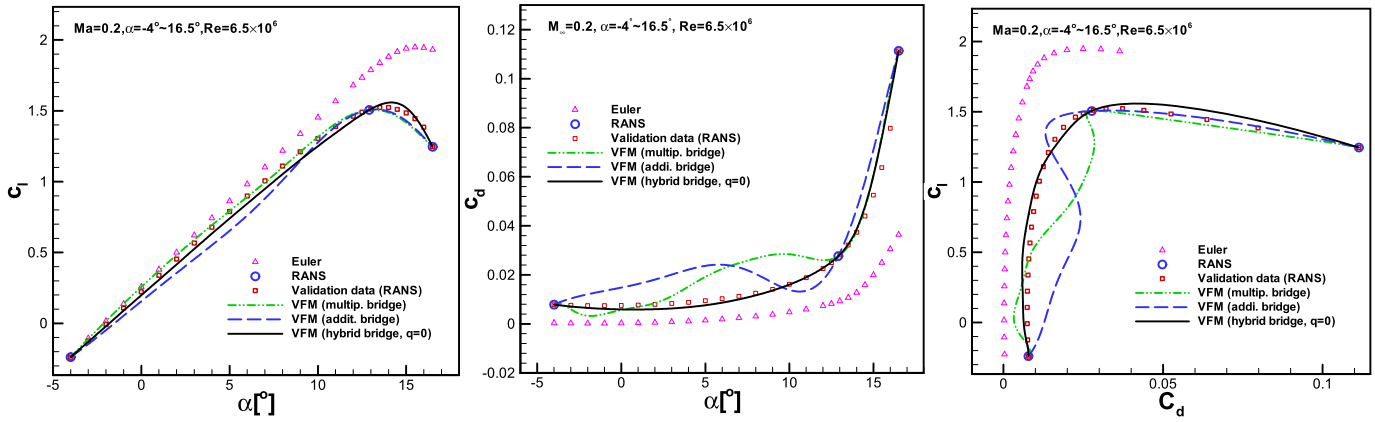

Fig. 10. Comparisons of different bridge functions for VFM of lift, drag and drag polar of RAE 2822 airfoil. (For interpretation of the references to color in this figure, the reader is referred to the web version of this article.)

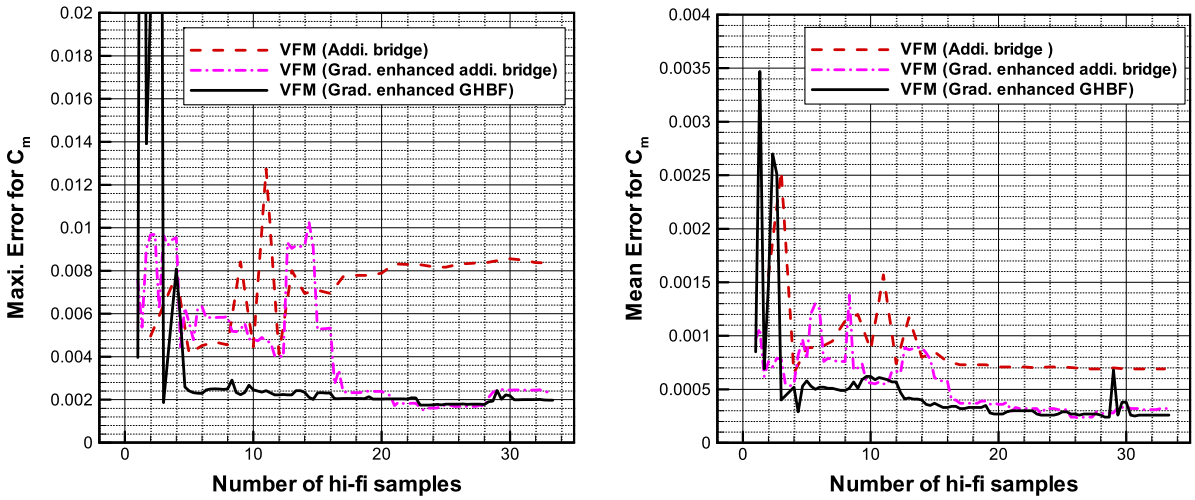

Fig. 11. Accuracy of VFM models for moment coefficient versus number of NS sample points considered (left: maximum error; right: mean error).

VFM follows the trend of the validation data. The example shows that the choice of bridge function has a dramatic effect on VFM, and that the GHBF is very promising. Note that as few as three high-fidelity samples, together with the low-fidelity samples, are sufficient to reproduce the non-linear functional relationship of the aerodynamic coefficients as a function of one parameter.

Note that the results can be further improved by performing adaptive sampling based on some error criterion, i.e. by iteratively adding samples in regions of the parameter space, where the functional relationship is highly non-linear. Such criteria for sample refinement have been developed by the authors but their presentation goes beyond the scope of this paper.

5.3. *Demonstration of gradient-enhanced Generalized Hybrid Bridge Function (GHBF)*

We consider again the RAE 2822 airfoil and use the gradient-enhanced GHBF to generate a VFM model for the moment coefficient as a function of two independent variables: angle of attack and Mach number. The Reynolds number was taken as 6.5×10^6. The angle of attack, α, and Mach number, *Ma*, were varied between $-4°$ to $8°$ and 0.1 to 0.5, respectively. The computational grids for Euler and Navier–Stokes computations with the DLR TAU code are shown in Fig. 8. We used a quasi-Monte Carlo approach [39] to sample the parameter space with 200 points for Euler computations and 2 to 35 points for the RANS computations (as well as viscous adjoint computations). A additional 200 Navier–Stokes (NS) computations were performed to obtain validation data.

Fig. 11 shows the accuracy of VFM models with varying the number of NS samples used. Note that for the gradient-enhanced approach, the gradients of the moment coefficient with respect to angle of attack and Mach number were computed via the corresponding viscous adjoint approach. When compared to the additive bridge function-based VFMs with and without gradients, the gradient-enhanced GHBF (black solid line) is the most accurate approach. For VFM with gradient-enhanced GHBF, 6 NS samples (including gradients) are sufficient to build an accurate surrogate model for the moment coefficient.

A more detailed comparison of different VFM models with a fixed number of NS samples (6 samples) is shown in Fig. 12 and Fig. 13. The 3D hyper surfaces of the moment coefficient are shown in Fig. 12. The comparison shows that the VFM with the gradient-enhanced GHBF (lower right figure) is the most accurate model. Gradient-information improves the accuracy of the additive bridge function in the highly non-linear region, but deteriorates in the linear region. Two slices of the hyper surfaces are shown in Fig. 13, for a Mach number of 0.45 and 0.5, respectively. In this figure, the difference between the different methods is shown more clearly. Additional NS computations were performed to validate the VFM models. The result of VFM with gradient enhanced GHBF (black solid line) is compared with kriging through only 6 NS samples (blue dash-double-dotted line), and VFMs with an additive bridge function (red dashed line) and a gradient-enhanced additive bridge

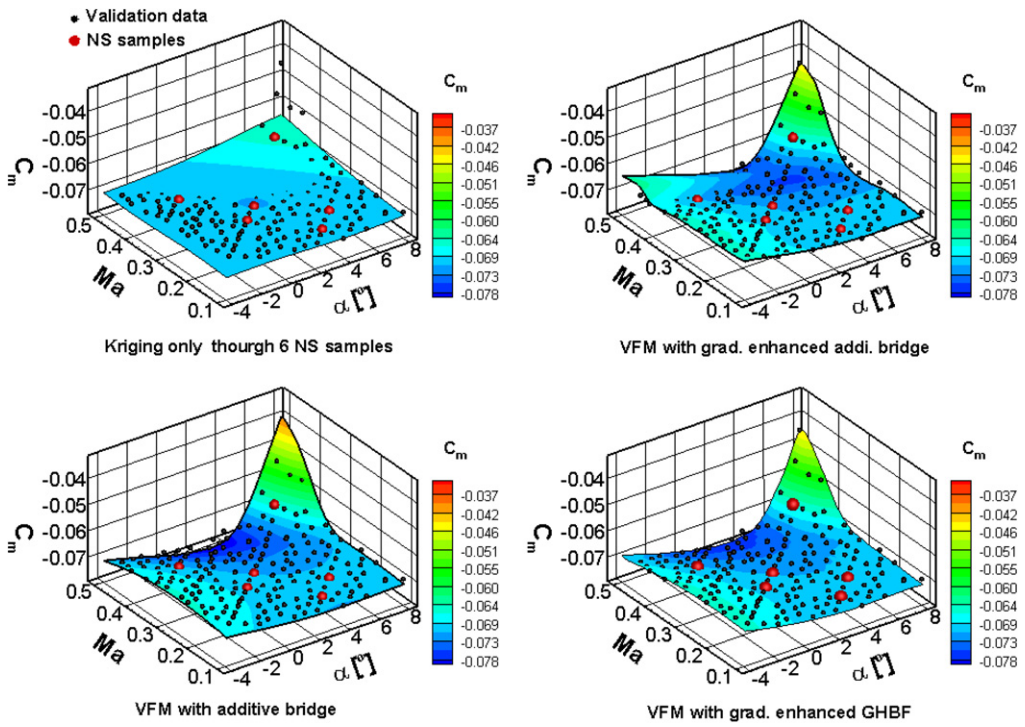

Fig. 12. Comparison of VFM models with validation data (black spheres, 200 NS samples) for the moment coefficient of the RAE 2822 airfoil as a function of angle of attach and Mach number; the 6 NS samples are denoted by red spheres. (For interpretation of the references to color in this figure legend, the reader is referred to the web version of this article.)

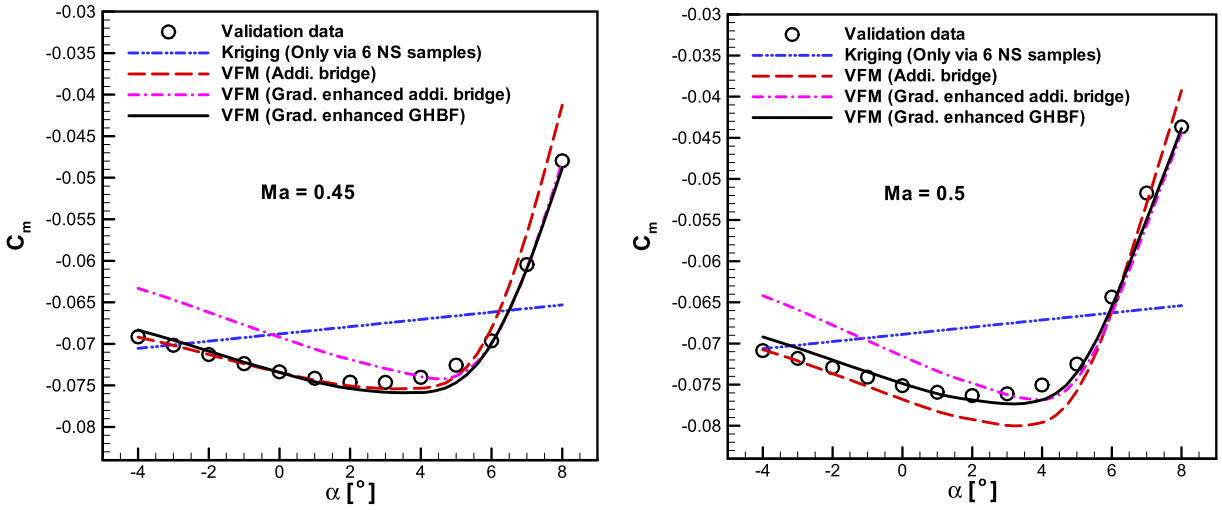

Fig. 13. Comparison of the various VFM models with the validation data (black circles, 13 NS samples) for the moment coefficient of the RAE 2822 airfoil at a constant Mach number of 0.45 and 0.5, respectively. (For interpretation of the references to color in this figure, the reader is referred to the web version of this article.)

function (pink dash-dotted line). The comparison shows that the VFM with a gradient enhanced GHBF is the most accurate approach for this example.

6. Conclusions

A Gradient-Enhanced Kriging (GEK) method combined with a new Generalized Hybrid Bridge Function (GHBF) was developed and investigated, aiming to improve the efficiency and accuracy of Variable-Fidelity Modeling (VFM). The developed algorithms and technologies were verified based on analytical problems and demonstrated for modeling the aerodynamic data of an RAE 2822 airfoil. Some conclusions can be drawn as follows:

- GEK provides a very promising means of significantly improving the accuracy of kriging for a given number of samples. When this method is coupled with the adjoint method, a very efficient method can be obtained for overcoming the problems associated with high-dimensional problems. In some cases, direct GEK is actually more accurate and easier to use than indirect GEK in spite of the fact that its derivation is more complicated.
- The GHBF method proposed in this paper is very promising for the construction of VFM models. It is essentially a generalization of additive and multiplicative bridge functions. Examples show that it is efficient and accurate for variable-fidelity surrogate modeling problems.

- Gradient-enhanced GHBF, combining GEK and GHBF methods, is demonstrated to be the most promising method. The accuracy, efficiency and robustness of building a variable-fidelity surrogate model of aerodynamic data can be improved significantly.

These new algorithms and technologies will be used to construct efficient and accurate VFM models for more industry-relevant problems. The relationship between the current VFM method and the cokriging method will be studied to derive a single mathematical model for the current VFM. Some theoretical issues such as the uncertainty estimation for VFM will be further investigated. Also, a mathematical model including CFD data of more than two levels of fidelities will be derived. A VFM that is able to take data from different data sources such as CFD, wind-tunnel data and flight test data will also be studied. New adaptive sample refinement strategies based on the ideas of Expected Improvement (EI), Lower Confidence Bounding (LCB) or other methods will be investigated to obtain an adaptive VFM that requires a minimum number of high-fidelity samples for a given accuracy. The next major step in the aero-data for loads context is the extension of the current VFM method to modeling distributed loads data for the elastic aircraft.

Acknowledgements

This research was sponsored by European Regional Development Fund, Economic Development Fund of the Federal German State of Lower Saxony, contract/grant number: W3-80026826.

The first author also benefited from the support of the National Natural Science Foundation of China (NSFC) under grant No. 10902088 and the Aeronautical Science Foundation of China under grant No. 2011ZA53008

References

[1] Z.-H. Han, S. Goertz, R. Hain, A variable-fidelity modeling method for aero-loads prediction, in: A. Dillmann, G. Heller, M. Klaas, H.-P. Kreplin, W. Nitsche, W. Schröder (Eds.), New Results in Numerical and Experimental Fluid Mechanics VII, in: Notes on Numerical Fluid Mechanics and Multidisciplinary Design, vol. 112, Springer, 2010, pp. 17–25.

[2] Z.-H. Han, R. Zimmermann, S. Goertz, A new cokriging method for variable-fidelity surrogate modeling of aerodynamic data, AIAA Paper 2010-1225, in: 48th AIAA Aerospace Sciences Meeting Including the New Horizons Forum and Aerospace Exposition, Orlando, FL, Jan. 4–7, 2010.

[3] K.J. Chang, R.T. Haftka, G.L. Giles, P.-J. Kao, Sensitivity-based scaling for approximating structural response, Journal of Aircraft 30 (2) (1993) 283–288.

[4] N.M. Alexandrov, R.M. Lewis, C.R. Gumbert, L.L. Green, P.A. Newman, Optimization with variable-fidelity models applied to wing design, AIAA Paper 2000-0841, Jan. 2000.

[5] N.M. Alexandrov, E.J. Nielsen, R.M. Lewis, W.K. Anderson, First-order model management with variable-fidelity physics applied to multi-element airfoil optimization, AIAA Paper 2000-4886, Sep. 2000.

[6] N.M. Alexandrov Jr., J.E. Dennis, R.M. Lewis, V. Torczon, A trust-region framework for managing the use of approximation models in optimization, Structural and Multidisciplinary Optimization 15 (1) (1998) 16–23.

[7] R.M. Lewis, S.G. Nash, A multigrid approach to the optimization of systems governed by differential equations, AIAA Paper 2000-4890, 2000.

[8] S. Choi, J.J. Alonso, I.M. Kroo, M. Wintzer, Multi-fidelity design optimization of low-boom supersonic business jets, AIAA Paper 2004-1530, 2004.

[9] S. Choi, J.J. Alonso, S. Kim, I. Kroo, M. Wintzer, Two-level multi-fidelity design optimization studies for supersonic jets, AIAA Paper 2005-0531, in: 43rd Aerospace Sciences Meeting and Exhibit, Reno, Nevada, Jan. 10–13, 2005.

[10] C.Y. Tang, K. Gee, S.L. Lawrence, Generation of aerodynamic data using a design of experiment and data fusion approach, AIAA Paper 2005-1137, Jan. 2005.

[11] S.E. Gano, J.E. Renaud, B. Sanders, Variable fidelity optimization using a kriging based scaling function, AIAA Paper 2004-4460, Aug. 2004.

[12] S.E. Gano, J.E. Renaud, J.D. Martin, T.W. Simpson, Update strategies for kriging models for using in variable fidelity optimization, AIAA Paper 2005–2057, April 2005.

[13] M.S. Eldred, A.A. Giunta, S.S. Collis, N.A. Alexandrov, R.M. Lewis, Second-order corrections for surrogate-based optimization with model hierarchies, AIAA Paper 2004-4457, Aug. 2004.

[14] D.G. Krige, A statistical approach to some basic mine valuations problems on the Witwatersrand, Journal of the Chemical Metallurgical and Mining Engineering Society of South Africa 52 (6) (1951) 119–139.

[15] G.M. Matheron, Principles of geostatistics, Economic Geology 58 (8) (1963) 1246–1266.

[16] H.-S. Chung, J.J. Alonso, Design of a low-boom supersonic business jet using cokriging approximation models, AIAA Paper 2002-5598, 2002.

[17] H.-S. Chung, J.J. Alonso, Using gradients to construct cokriging approximation models for high-dimensional design optimization problems, AIAA Paper 2002-0317, Jan. 2002.

[18] W. Liu, S.M. Batill, Gradient-enhanced response surface approximations using kriging models, AIAA Paper 2002-5456, 2002.

[19] W. Liu, Development of gradient-enhanced kriging approximations for multidisciplinary design optimization, Ph.D. thesis, University of Notre Dame, Notre Dame, IN, USA, 2003.

[20] J. Laurenceau, P. Sagaut, Building efficient response surfaces of aerodynamic functions with kriging and cokriging, AIAA Journal 46 (2) (2008) 498–507.

[21] A.I.J. Forrester, A. Keane, Recent advances in surrogate-based optimization, Progress in Aerospace Sciences 45 (1–3) (January–April 2009) 50–79.

[22] R. Dwight, Z.-H. Han, Efficient uncertainty quantification using gradient-enhanced kriging, AIAA Paper 2009-2276, in: 11th AIAA Non-Deterministic Approaches Conference, Palm Springs, California, May 4–7, 2009.

[23] J. Sacks, W.J. Welch, T.J. Mitchell, H.P. Wynn, Design and analysis of computer experiments, Statistical Science 4 (4) (1989) 409–435.

[24] S.N. Lophaven, H.B. Nielsen, J. Søndergaard, Aspects of the Matlab Toolbox DACE, Technical Report IMM-REP-2002-13, Informatics and Mathematical Modelling, Technical University of Denmark, 2002; http://www2.imm.dtu.dk/~hbn/dace/.

[25] J. Kowalik, M.R. Osborne, Methods for Unconstrained Optimization Problems, Elsevier, New York, USA, 1968.

[26] A.G. Journel, C.J. Huijbregts, Mining Geostatistics, Academic Press, London, 1978.

[27] Y. Kuya, K. Takeda, X. Zhang, A.I.J. Forrester, Multifidelity surrogate modeling of experimental and computational aerodynamic data sets, AIAA Journal 49 (2) (February 2011) 289–298.

[28] R. Zimmermann, Z.-H. Han, Simplified cross-correlation estimation for multi-fidelity surrogate cokriging models, Advances and Applications in Mathematical Sciences 7 (2) (2010) 181–201.

[29] Z.-H. Han, S. Goertz, R. Zimmermann, On improving efficiency and accuracy of variable-fidelity surrogate modeling in aero-data for loads context, in: Proceeding of CEAS 2009 European Air and Space Conference, Manchester, UK, Oct. 26–29, 2009.

[30] A. Jameson, Optimum aerodynamic design using CFD and control theory, AIAA Paper 95-1729-CP, 1995.

[31] D.J. Mavripilis, A discrete adjoint-based approach for optimization problems on three-dimensional unstructured meshes, AIAA Paper 2006-50, 2006.

[32] M. Galle, T. Gerhold, J. Evans, Parallel computation of turbulent flows around complex geometries on hybrid grids with the DLR-TAU code, in: A. Ecer, D.R. Emerson (Eds.), Proc. 11th Parallel CFD Conf., Williamsburg, VA, May 23–26, 1999, North-Holland, 1999.

[33] T. Gerhold, V. Hannemann, D. Schwamborn, On the validation of the DLR-TAU code, in: W. Nitsche, H.-J. Heinemann, R. Hilbig (Eds.), New Results in Numerical and Experimental Fluid Mechanics, in: Notes on Numerical Fluid Mechanics, vol. 72, Vieweg, ISBN 3-528-03122-0, 1999, pp. 426–433.

[34] N. Kroll, J.K. Fassbender (Eds.), MEGAFLOW – Numerical Flow Simulation for Aircraft Design, Notes on Numerical Fluid Mechanics and Multidisciplinary Design, vol. 89, Springer, 2005.

[35] D. Schwamborn, T. Gerhold, R. Heinrich, The DLR TAU-code: Recent applications in research and industry, invited lecture, in: P. Wesseling, E. Oate, J. Priaux (Eds.), Proceedings of the European Conference on Computational Fluid Dynamics (ECCOMAS CFD 2006), The Netherlands, 2006, on CD.

[36] R. Dwight, J. Brezillon, D. Vollmer, Efficient algorithms for solution of the adjoint compressible Navier–Stokes equations with applications, in: Proceedings of ONERA-DLR Aerospace Symposium (ODAS), Toulouse, October 2006.

[37] R. Dwight, J. Brezillon, Effect of approximations of the discrete adjoint on gradient-based optimization, AIAA Journal 44 (12) (2006) 3022–3071.

[38] R. Dwight, J. Brezillon, Adjoint algorithms for the optimization of 3d turbulent configurations, in: C. Tropea, et al. (Eds.), New Results in Numerical and Experimental Fluid Mechanics VI, in: Notes on Numerical Fluid Mechanics and Multidisciplinary Design, vol. 96, Springer, Heidelberg, 2008, pp. 194–201.

[39] C. Lemieux, Monte Carlo and Quasi-Monte Carlo Sampling, Springer Series in Statistics, Springer, New York, 2009.